Quantum Electronics **36** (8) 778 – 784 (2006)

LASER BEAMS

PACS numbers: 42.65.Es; 42.60.Jf
DOI: 10.1070/QE2006v036n08ABEH013275

On the reconstruction of parameters of quasi-Gaussian pump beams during transient SBS

A.S. Dementjev, E.K. Kosenko, E. Murauskas, V. Girdauskas

***Abstract*. The radii and radii of curvature of Stokes stimulated Brillouin scattering (SBS) beams are measured by the method of moments for smooth nearly Gaussian focused pump beams with the propagation ratio $M_{\sigma p}^2 \leqslant 1.2$. It is shown that in the case of sufficiently deeply focused pump radiation, the propagation ratio $M_{\sigma S}^2$ of Stokes beams near the threshold of the transient SBS is smaller than $M_{\sigma p}^2$ and approaches it with increasing the pump pulse energy. It is also found that the radii of Stokes beams at the output from a nonlinear medium are smaller than the radii of pump beams, while the radii of wave-front curvature are close (in modulus) to the radii of wave-front curvature for pump beams.**

Keywords: *stimulated Brillouin scattering, laser beams, beam propagation ratio.*

1. Introduction

Phase conjugation (PC) was discovered in 1971 in the study of stimulated scattering of light by hypersound and is described in detail in monographs and reviews [1 – 6]. Even earlier, it was found in some experiments with smooth beams (see [1 – 6] and references therein) that the divergence of stimulated backscattered radiation was close to that of the exciting radiation. Because the direct measurement of the intensity distributions and wave fronts (WFs) in the exciting and Stokes beams still involves some difficulties, it was proposed to demonstrate clearly PC upon stimulated Brillouin scattering (SBS) by placing into the diffraction-quality exciting beam a 'chaotic' phase plate prepared by etching a plane – parallel glass plate in hydrofluoric acid [5]. In this way, the detection of PC beams with a complicated WF shape was reduced to the measurements of the divergence and diameters of the exciting and reflected beams.

Note that without placing amplitude transparencies into a pump beam it is difficult to make conclusions about the reproducibility of the near-field spatial distributions of the pump beam amplitude based only on far-field measurements of energy fractions within given angles [4, 7]. However, it is considered traditionally that 'phase conjugation in a nonlinear medium is a physical process induced by the incident wave which results in the formation of a new wave directed towards the initial wave and having the same amplitude distribution but conjugated phase' [2]. Therefore, by using terms 'phase conjugation' and 'wave front reversal', we consider not only the WF phase of the reflected beam but also its amplitude. For coherent beams with smooth phase and amplitude distributions, this can lead to some misunderstandings. Thus, it was shown in the fixed field approximation for a Gaussian pump beam [8] that the scattered beam at the output from a nonlinear medium is narrower than the pump beam and its radius of curvature at deep focusing tends asymptotically to the radius of WF curvature of pump radiation. However, the reconstruction of the WF curvature is not PC in the traditional treatment [9].

Phase conjugate laser systems with SBS pulse compression are already commercially produced and widely used at present [10]. Note, however, that phase plates are seldom used in such systems because they either reduce the efficiency of the system or do not allow, for example, pulse compression. Therefore, the problem of a change in the parameters of smooth beams after reflection from a SBS mirror remains of current interest in the development of PC laser systems with pulse compression.

The international standard organisation recommends the measurements of the radius and angular divergence of beams by the method of second moments of the energy density distribution in the beam cross section [11, 12]. The WF surface is also determined by measuring the energy density distribution in the beam cross section [13, 14].

In this paper, we compare the parameters of the pump and Stokes beams upon transient SBS measured by the method of moments. This method was realised by producing an additional waist in the pump beam in front of a focusing lens of the SBS mirror. The corresponding waist in the Stokes beam was formed automatically. By measuring with a CCD camera the energy density distributions in the sufficient number of beam cross sections along the propagation direction of the laser and Stokes beams using the original software package [15], we determined the waist size and position for the so-called embedded Gaussian beams [16 – 18] and calculated propagation ratios M_σ^2 for the laser and Stokes beams. These results allow us to calculate and compare the generalised radii and radii of curvature of the laser and Stokes beams in the input plane of the SBS mirror

A.S. Dementjev, E.K. Kosenko, E. Murauskas Nonlinear Optics and Spectroscopy Laboratory, Institute of Physics, Savanoriu av. 231, LT-02300 Vilnius, Lithuania; e-mail: aldement@ktl.mii.lt;
V. Girdauskas Physics Department, Vytautas Magnus University, Vileikos 8, LT-44404 Kaunas, Lithuania

Received 25 January 2006; revision received 27 April 2006
Kvantovaya Elektronika **36** (8) 778 – 784 (2006)
Translated by M.N. Sapozhnikov

and, therefore, to estimate the accuracy of reproducibility of the parameters of smooth quasi-Gaussian pump beams.

2. Statement of the experiment

The parameters of the pump and Stokes beams are usually compared by measuring their near-field sizes and the far-field angular radiation distribution. In most cases, a lens focusing pump radiation is located directly at the input to a nonlinear medium. The focusing lens can be placed at a rather long distance from the SBS cell; however, the positions of the lens and measurements planes of the corresponding parameters are not always distinctly indicated.

We used the method of moments for measuring the parameters of the laser and Stokes beams such as the radii of beam waists and positions of planes in which they are located and the propagation ratios M_σ^2 of the beams. Note that the generalised radius $w_\sigma(z)$ of the beam, the radius of curvature $R_\sigma(z)$ and the complex parameter

$$\frac{1}{q_\sigma} = \frac{1}{R_\sigma} + \frac{\mathrm{i}\lambda M_\sigma^2}{\pi w_\sigma^2} \tag{1}$$

of the beam in a free space determined by the method of moments (see, for example, [16–18] and references therein) satisfy the corresponding relations for Gaussian beams [19], in particular, for the angular divergence θ_σ:

$$\theta_\sigma = \frac{w_\sigma}{|q_\sigma|} = \left[\left(\frac{w_\sigma}{R_\sigma}\right)^2 + \left(\frac{\lambda M_\sigma^2}{\pi w_\sigma}\right)^2\right]^{1/2} = \frac{\lambda M_\sigma^2}{\pi w_{\sigma 0}}, \tag{2}$$

where λ is the wavelength in vacuum; $M_\sigma^2 = 1$ for Gaussian beams; and $w_{\sigma 0}$ is the radius of the beam in a real or 'imaginary' waist.

Note that the generalised radii of curvature R_σ determined by the method of moments [16–18] coincide with the radii of curvature of paraboloid surfaces approximating the WF surface according to the ISO-15367-1 standard [13]. Therefore, the generalised radii R_σ of WF curvature in different cross sections of the beam calculated from experimentally measured ratios M_σ^2 correspond to the requirements of the standard [13]. For Gaussian beams, the paraboloid surfaces and radii of curvature approximating the WF according to the standard [13] coincide with usual ones [16, 17]. Recall that embedded Gaussian beams are not necessarily real beams for which the beam radius is determined in each plane by the relation $w_{\sigma\mathrm{emb}} = w_\sigma / M_\sigma$ (see [18] and references therein).

Thus, according to (2), the total angular divergence of a beam is determined by the so-called geometrical ($\theta_{\sigma\mathrm{g}} = w_\sigma/|R_\sigma|$) and diffraction [$\theta_{\sigma\mathrm{d}} = \lambda M_\sigma^2/(\pi w_\sigma)$] divergences of the beam [19]. Let us discuss this question in more detail by using the expressions for the radius and radius of WF curvature for scattered radiation obtained in [8] in the fixed field approximation for a Gaussian pump beam:

$$\tilde{w}_\mathrm{S}(z) = \beta w_\mathrm{p}(z), \quad \tilde{R}_\mathrm{S}(z) = -\alpha(\beta, z) R_\mathrm{p}(z), \tag{3}$$

where coefficients $0 < \beta < 1$ and $0 < \alpha(\beta, z) < 1$ depend on the parameters of the pump beam. The quantities with the tilde correspond to the Stokes beam in a SBS medium, which differs from a usual Gaussian beam in a linear medium. The solution for the Stokes beam propagating in the positive direction along the z axis obtained in [8] is a Gaussian beam in each section of the nonlinear medium, however, its parameters (beam radius, radius of curvature, intensity, etc.) change differently than in free space. Indeed, the position of the minimal radius of this beam in the medium coincides with that of the waist of a 'normal' Gaussian pump beam, which is, however, is not the beam waist in its standard definition. Only at the output from the SBS medium, this beam transforms to a 'normal' Gaussian beam and its parameters are finally formed. It follows from expressions obtained in [8] that for $z \gg z_\mathrm{d} = k w_\mathrm{p}^2(0)/2$ (where k is the wave number; the pump beam waist is located in the plane $z = 0$), the WF of scattered radiation reproduces quite accurately $[\alpha(z) \to 1]$ the WF of the Gaussian pump beam: $|R_\mathrm{S}(z)| = |-R_\mathrm{p}(z)|$.

First we will analyse the angular dependence of scattered radiation, which is required for a correct statement of the experiment, for the simplest case when a Gaussian pump beam with a plane WF is incident on the SBS mirror lens located directly at the cell input. Then, the WF of scattered radiation propagated through the lens also becomes plane at the output from the nonlinear medium if it is perfectly reconstructed. However, because of the radial compression ($w_\mathrm{S} < w_\mathrm{p}$) of the scattered beam [8], its angular divergence $\theta_\mathrm{S} = \lambda/(\pi w_\mathrm{S})$, which is determined in this case only by the diffraction part, is higher than that of the pump beam incident on the SBS mirror lens. Therefore, the far-field ($d \gg d_\mathrm{S}$) transverse size of the Stokes beam will exceed that of the pump beam. Here, d is the distance from the focusing lens of the SBS mirror to the measurement plane and $d_\mathrm{S} = \pi w_\mathrm{S}^2/\lambda$ is the diffraction length of the Stokes beam taking into account that the radiation wavelength upon SBS changes very weakly. On the contrary, the radius of pump beams measured in the near field ($d \leqslant d_\mathrm{S}$) will exceed the radius of the Stokes beam.

In the case of a nonplanar WF of the pump beam on the focusing lens located close to the cell, the situation is more complicated. Because $|R_\mathrm{S}| \leqslant |R_\mathrm{p}|$ [8], the geometrical part $\theta_{\mathrm{S}\,\mathrm{g}} = w_\mathrm{S}/|R_\mathrm{S}|$ of the divergence of Stokes radiation (rather than the total divergence, as is implicitly assumed in [8]) at the output from the SBS medium is lower than the geometrical divergence of the pump beam. The question about the total divergence of the Stokes beam determined by expression (2) requires a detailed discussion.

Consider first for simplicity a Gaussian pump beam ($M_\sigma^2 = 1$, $\lambda = 1.064$ μm), which can have different radii of curvature on a focusing lens. Figure 1 shows the dependences of the total divergence of this beam on its radius calculated by expression (2) for three radii of curvature. For the specified radius of WF curvature R_σ, the total divergence of the beam is minimal for the beam radius $w_\sigma = (\lambda|R_\sigma|/\pi)^{1/2}$. Therefore, the reconstruction of the radius of WF curvature and a decrease in the Stokes beam radius can result (upon preservation of the propagation ratio $M_\sigma^2 = 1$), depending on the radius of curvature of the pump beam, both in the decrease and increase of the total divergence of the Stokes beam compared to the pump beam (points P_1, P_2, P_3 in Fig. 1 correspond to the pump beam and points S_1 S_2, S_3 – to the Stokes SBS beam). For small radii of curvature ($|R_\sigma| < \pi w_\sigma^2/\lambda$), the angular divergence is mainly determined by its geometrical part – the right part of curve (*1*) (Fig. 1). As a result, the total angular divergence of the Stokes beam in this case is lower than the angular divergence of the pump beam. It is this situation that is

usually realised behind the focusing lens with the focal distance $f < \pi w_p^2/\lambda$. For this reason, although not always, as claimed in [8], but usually the divergence of the Stokes beam at the output from the SBS medium (in front of the lens) is lower than that of the pump beam (if the condition $z \gg z_d$ is fulfilled). Behind the focusing lens, the divergence of the Stokes beam (Fig. 1) can be both lower [when the radii of curvature of the pump beam are small enough (points P_1 and S_1)] and higher (points P_3 and S_3) than the divergence of the pump beam. In addition, the situation is possible for certain radii of the beam and WF curvature when the divergences of the Stokes and pump beams do not differ noticeably (points P_2 and S_2). Note that when the radius of WF curvature is large [curve (*3*) in Fig. 1], the total angular divergence of the beam also has a minimum, which is achieved at a comparatively large radius of the beam (~ 6 mm).

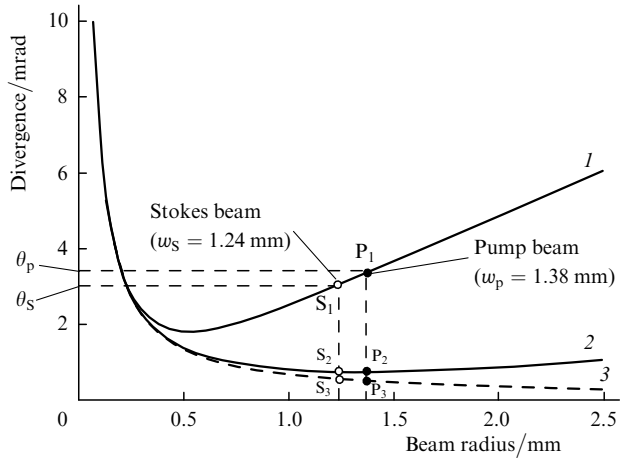

Figure 1. Angular divergences of the Gaussian beam as functions of the beam radius for the radii of WF curvature 0.829 (*1*), 5 (*2*), and 100 m (*3*).

We believe that the dependence of the total divergence of the Stokes beam on the radius of WF curvature of the pump beam was adequately studied already in paper [20]. However, relations of the type (1)–(3) were used in comparatively recent papers [10, 21, 22] not quite correctly, and it seems expedient to make some remarks. According to the above discussion, we can assume that upon SBS of Gaussian beams under certain conditions (for example, in the fixed-pump field approximation), the reversal of the WF curvature can be realised rather than the total phase conjugation of the pump beam. However, the requirement $|z| \gg z_d$ at which it is realised is often not remembered [8]. This requirement means that the pump beam waist should be located deeply enough inside the SBS mirror and its length should be much smaller than the distance to the output window of the SBS cell.

Due to the neglect of this requirement, the parameters of the SBS mirror such as the focal distance of a focusing lens, its position with respect to a cell, the cell size, etc. are not indicated in some papers. As a result, the requirement of deep enough focusing may be not fulfilled under certain experimental conditions. In this case, the WF curvature upon reflection from the SBS mirror should be determined by more general expression (3), from which it follows that the modulus of the radius of curvature of the Stokes beam is always smaller than the modulus of the radius of curvature of the pump beam and tends to it asymptotically with increasing the coordinate z of the output plane. Therefore, the geometrical and all the more total divergence of the Stokes beam can exceed the divergence of the pump beam.

Therefore, the radius of the Stokes beam on the focusing lens located at a large enough distance from the cell can exceed the radius of the pump beam. Such a situation with not deep focusing into the SBS cell ($z \geqslant z_d$) was specially realised in our experiments, and in this case the radius of the Stokes beam on the focusing lens considerably exceeded the pump-beam radius. It is possible that such conditions were realised, for example, in [21]. Therefore, one should bear in mind that not only the expression for the Stokes-beam radius in the ray matrix for the SBS mirror [10, 21–23] should depend on the parameter β but also the expression for its radius of curvature, which also depends in the general case on the ratio z/z_d [8].

We studied the accuracy of reconstruction of the parameters of the pump beam upon transient SBS by using the experimental setup shown schematically in Fig. 2. Pumping was performed by passively Q-switched single-mode Nd : YAG laser (*1*). Iris diaphragm (*2*) blocked a weak diffraction ring from the intracavity diaphragm used for the selection of the fundamental transverse mode. The laser pulse energy W_L was ~ 3.5 mJ and the pulse duration was $\tau_L \sim 3$ ns. The pump pulse energy could be continuously varied with the help of half-wave plate (*3*) and thin-filmed polariser (*4*). Spherical lens (*5*) produced the additional waist in the pump beam required for measurements of the propagation ratio. By selecting the focal distance of lens (*5*) and distances to SBS cell (*13*), we changed the parameters of the pump beam on focusing lens (*12*) placed close to cell (*13*). As a nonlinear medium, we used CCl_4, which is often employed in SBS mirrors and has the stimulated scattering threshold $W^* \sim 0.9$ mJ in our case.

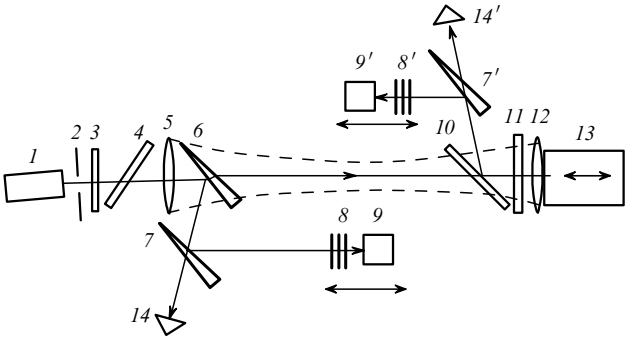

Figure 2. Scheme of the experimental setup for measuring the spatial parameters of the pump and Stokes beams upon the transient SBS of focused quasi-Gaussian beams: (*1*) Nd : YAG laser; (*2*) diaphragm; (*3*) half-wave plate; (*4*) polariser; (*5*) spherical lens; (*6*) optical wedge; (*7, 7′*) additional optical wedges; (*8, 8′*) neutral filters; (*9, 9′*) CCD cameras; (*10*) polariser; (*11*) quarter-wave plate; (*12*) focusing lens; (*13*) cell; (*14, 14′*) photodiodes.

3. Experimental results and discussion

The parameters of pump pulses were measured at a pulse repetition rate of ~ 1 Hz. Because no changes in the

parameters of the incident and reflected pulses were observed with time at this repetition rate, the measurements were performed successively: first for pump pulses and then for reflected pulses. Indication optical wedge (*6*) directed a part of radiation to calibration photodiode (*14*) to measure the pump pulse energy. After reflection from additional optical wedge (*7*), a part of the pump radiation propagated through neutral filters (*8*) and was incident to CCD camera (*9*) to measure spatial parameters. Thin-filmed dielectric polariser (*10*) and quarter-wave plate (*11*) were used to couple Stokes radiation to a similar arm to measure the spatial characteristics of the Stokes beam. Sets of neutral filters (*8, 8'*) were used to provide the linear operating regime of the CCD camera.

The energy density distributions over the Stokes and pump beam cross sections was measured with an Electrim 1000N CCD camera according to the requirements of the standard [12]. The experimental data were processed by using the original software package [15]. The transverse distribution of pump radiation was smooth and close to that of the TEM_{00} mode (the propagation ratio of the beam was $M^2_{\sigma p} \approx 1.2$). The transverse distribution of the energy density of Stokes beams was also smooth.

Figure 3 shows the energy-density distributions in the cross section of the Stokes beam along axes x and y in one of the measurement planes (the corresponding line and column in the CCD camera intersect near the maximum of the beam energy density). One can see that the energy density distribution is axially symmetric and smooth (close to Gaussian). This allows us to use the ISO standard [12] for stigmatic beams and the corresponding definitions for beam radii w_σ [18].

As mentioned above, spherical lens (*5*) (Fig. 2) was used to measure the parameters of the pump beam at the input to the SBS mirror consisting of spherical lens (*12*) and quartz cell (*13*) filled with CCl_4 liquid, which was additionally purified. First the pump beam was formed with a waist in the plane of lens (*12*) with a focal distance of 100 mm. Figure 4 shows the results of measurements of radii of pump and Stokes beams along the propagation direction of the beams [the origin of the z axis is made coincident with the position of lens (*5*)] for two laser pulse energies. One can see that for both pump energies the radii of Stokes beams on the lens (whose position is indicated by the dashed straight line) are smaller than the pump-beam radius. At the same time, by selecting the measurement plane for the Stokes beam at some distance d from focusing lens (*12*), we can obtain the beam diameter greater than that of the pump beam. Calculations of the radii and radii of curvature of beams by the method of moments from the expressions

$$w_\sigma(z) = w_{\sigma 0}\left\{1 + \left[\frac{\lambda M^2_\sigma (z - z_{\sigma 0})}{\pi w^2_{\sigma 0}}\right]^2\right\}^{1/2}, \tag{4}$$

$$|R_\sigma(z)| = |z - z_{\sigma 0}|\left\{1 + \left[\frac{\pi w^2_{\sigma 0}}{\lambda M^2_\sigma (z - z_{\sigma 0})}\right]^2\right\}, \tag{5}$$

where $w_{\sigma 0}$ and $z_{\sigma 0}$ are the radius and position of the waist of the beam with the propagation ratio M^2_σ, show that the waists of the beams propagated through lens (*12*) are located behind it (on the cell side), and the WF of Stokes beams propagated through the lens are no longer plane.

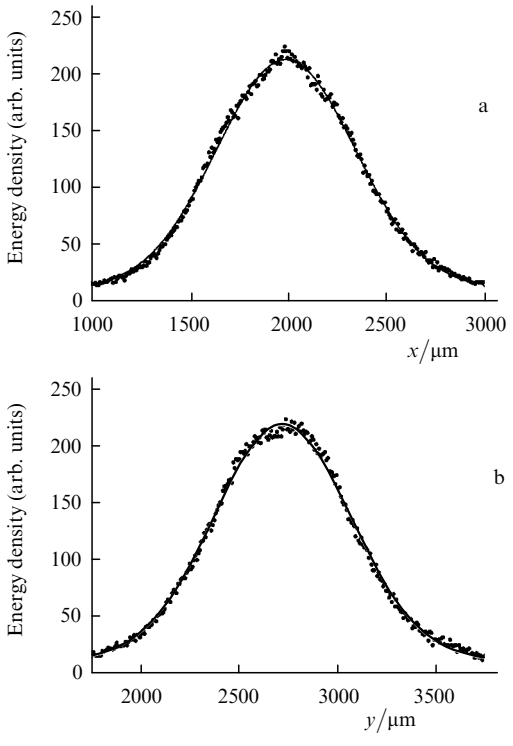

Figure 3. Energy density distributions over the coordinates x (a) and y (b) in the Stokes-beam cross section.

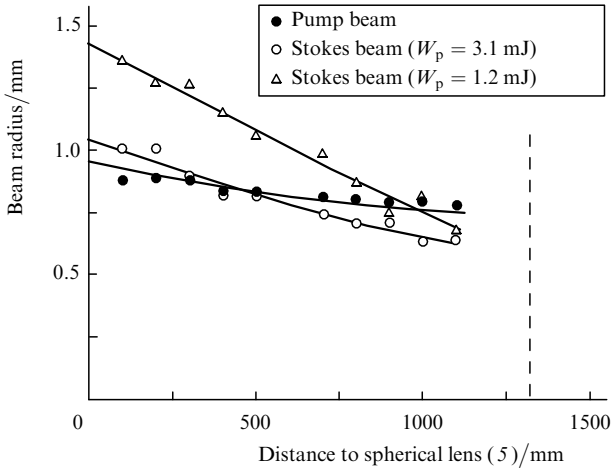

Figure 4. Radii of the pump and Stokes beams for different pump-pulse energies as functions of the distance to lens (*5*) in the case when the pump-beam waist is located on lens (*12*) whose position is indicated by the dashed straight line.

However, the measurement of the position and radius of the Stokes-beam waist is not accurate in this case because upon such pumping geometry the radii of the Stokes beam can be measured only from one side of the waist. For this reason, an additional waist was formed with the help of lens (*5*), which was located at a large enough distance from lens (*12*), which allowed us to measure the total caustic of Stokes beams. In this case, the focal distance of lens (*12*) was 120 mm. Figure 5 presents the beam radii measured for two pump energies. These experimental data were approximated by expression (4). The positions and radii of waists and propagation ratios M^2_σ were determined by the method

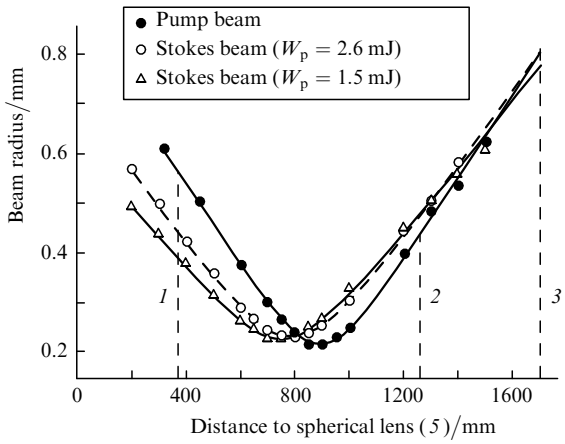

Figure 5. Radii of the pump and Stokes beams for different pump-pulse energies as functions of the distance to lens (*5*) in the case when the radius of curvature of the diverging pump beam on lens (*12*) whose position is $R_{\sigma p} = 832$ mm; dashed straight lines (*1*) and (*2*) indicate the positions of darkening discs; dashed straight line (*3*) indicates the position of lens (*12*).

of least squares, and the angular divergence of beams was determined by expression (2). The values of these parameters are presented in Table 1.

One can see from Table 1 that the propagation ratio M_σ^2 for the Stokes beam is lower than that for the pump beam when the SBS threshold is slightly exceeded and increases with increasing the pump pulse energy, approaching the propagation ratio of the pump beam. In this case, the position of the Stokes-beam waist does not coincide with that of the pump beam and is displaced toward the pump laser when the pump energy is close to the SBS threshold. An increase in the pupm pulse energy leads to the approach of the Stokes-beam waist with that of the pump beam.

By using the parameters of beams presented in Table 1, we can determine from (5) the generalised radii of WF curvature of the beams on focusing lens (*12*) (on the pump laser side). The radius of WF curvature for the pump beam was $R_{\sigma p} = 832$ mm. For the pump energy W_p close to the threshold ($W_p = 1.7W^*$), the radius of WF curvature of the Stokes beam propagated through lens (*12*) in the opposite direction was $R'_{\sigma S} = -991$ mm, and when the pump energy exceeded the threshold by a factor of ~ 2.9, this radius was -943 mm. By using the expression $1/R'_\sigma = 1/R_\sigma - 1/f$ for the transformation of the radius of WF curvature for a thin spherical lens (where R_σ and R'_σ are the radii of WF curvature at the lens input and output) [16], we can calculate the radii of WF curvature of beams at the input to a nonlinear medium. Table 1 presents the radii of WF curvature calculated in front and behind the focusing lens.

One can see that the modulus of the radius of WF curvature of the Stokes beam at the output from the medium differs by no more than 3 % from the modulus of the radius of WF curvature of the pump beam at the input to the medium. The detection of such small differences between the radii of WF curvature in direct near-field measurements by using, for example, Shack–Hartmann sensors [14] involves considerable difficulties. Because of this, the accuracy of PC is often estimated by measuring a part of energy propagating through a certain aperture or, vice versa, bypassing a darkening disc [9]. One can see from Fig. 5 that the Stokes-beam radius at the output from a nonlinear medium is smaller than the pump-beam radius and approaches it with increasing pump energy. The beam radii on lens (*12*) calculated by expression (4) are presented in Table 1. However, depending on the choice of the position of the measurement plane, the Stokes-beam radius can be either larger or smaller than the pump-beam radius. Thus, a darkening disc placed to the position conjugate to position (*1*) in Fig. 5 would not transmit in fact the Stokes beams. At the same time, a considerable part of the Stokes-pulse energy would bypass the darkening disc placed in position (*2*). Therefore, generally speaking, the fraction of energy of 'nonreversed radiation' measured in [9] with the help of a darkening disc is not a reliable (unambiguous) parameter of the PC quality. Of course, SBS upon broadband pumping has its own features [9, 24, 25]. However, we suppose that the statement that 'the Stokes beam is broadened at the output from the medium compared to the pump beam' made in [9] based on indirect measurements is not adequately substantiated.

Note also that the authors of paper [26] report, with reference to [9], that numerical calculations did not reveal any considerable increase in the width of the scattered beam compared to that of the incident beam, which is typical for PC upon broadband pumping. Our numerical calculations performed for the stationary [20] and transient [27–30] SBS of focused Gaussian beams in the generation regime beginning from the spontaneous scattering noise showed that the normalised energy density distributions of Stokes pulses at the output from a medium are always narrower than those for pump pulses. However, there are papers [31, 32] in which numerical calculations for narrowband pumping also give Stokes beams with a nearly Gaussian transverse distribution and the output radius exceeding that of the pump beam.

In [31], a stationary SBS of the focused Gaussian beam was considered and the expansion of fields in Hermite–Gaussian modes was used, and in [32] the transient SBS of long pulses was studied and the expansion of fields in Laguerre–Gaussian modes was used. It was reported in [31] that the Stokes-beam radius at the output from the medium near the threshold was greater than the pump-beam radius by a factor of 1.9, and for the tenfold excess over the threshold – by a factor of 1.3. The authors of paper [31] point out themselves that Stokes beams can be also narrower than the pump beam. It is possible that the result obtained in [31] is the consequence of approximations used in the numerical calculation. The beam radius at the output from the medium was calculated in [32] by the method of moments by using the time-averaged intensity. The results reported in [32] show that the Stokes-pulse radius is greater

Table 1. Parameters of the pump and Stokes beams.

Beam	W_p/mJ	M_σ^2	$w_{\sigma 0}$/mm	$z_{\sigma 0}$/mm	θ_σ/mrad	w_σ/mm	R_σ/mm	R'_σ/mm
pump	3.5	1.17	0.23	892	1.68	1.38	+832	−140
Stokes	1.5	1.07	0.26	745	1.39	1.35	−991	+137
Stokes	2.6	1.14	0.26	791	1.48	1.37	−943	+ 138

than that of the pump beam by a factor of 1.8. Note that the following papers [33, 34] with participation of the same authors do not present distinct information on the Stokes-beam radii.

Because the question about the relation between the radii of Stokes and laser beams at the output from the SBS medium is important, we present here briefly the results of numerical calculation of the Stokes-pulse radius determined by the expression

$$w_{\sigma S}(z,t) = 2\left[\frac{\pi}{P_S}\int_0^\infty r^3|e_S|^2 dr\right]^{1/2}, \quad (6)$$

where $e_S(r,z,t)$ is the slowly varying complex amplitude of the Stokes pulse. The expressions for the instant power $P_S(t)$ and propagation ratio $M^2_{\sigma S}(t)$ of the Stokes beam in terms of the complex amplitude $e_S(r,z,t)$ are presented in papers [18, 30]. The spatiotemporal structure of compressed Stokes pulses has a complicated shape [27–30], and therefore the instant power, radius, and propagation coefficient of the beam strongly change during the pulse. In this connection it is reasonable to introduce instead of instant values their time-averaged values with the instant power as the weight function. Then, the averaged radius of the beam is described by the expression

$$\langle w_{\sigma S}(t)\rangle = \int_{-\infty}^{\infty} w_{\sigma S}(t)P_S(t)dt \Big/ \int_{-\infty}^{\infty} P_S(t)dt$$

and the averaged propagation ratio $\langle M^2_{\sigma S}(t)\rangle$ is determined similarly [30].

The time dependences of the power, radius, and propagation ratio of the Stokes beam at the output from a nonlinear medium are presented in Fig. 6 where the values of averaged parameters are also given. The calculations were performed by using the algorithm and program described in [30] for heavy Freon as the SBS medium and the pump-pulse duration $\tau_p = 2$ ns, pulse energy $W_p = 4$ mJ, the Gaussian-beam radius on the lens $w_p = 1.4$ mm, and the focal distance of the lens $f = 19$ cm. One can see from Fig. 6 that the Stokes-beam radius in the SBS compression regime exceeds the pump-beam radius only in the trailing edge of pulses when the instant pulse power is low and the spatial distribution of its intensity is annular, thereby increasing the beam radius determined by the method of moments. For this reason, the time-averaged (with the instant power as the weight function) radius of the Stokes beam is considerably smaller than the pump-beam radius.

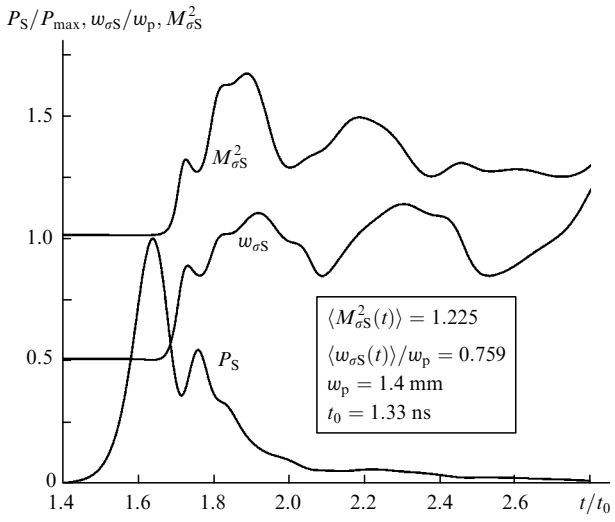

Figure 6. Time dependences of the normalised instant powers P_S, radius $w_{\sigma S}$, and propagation ratio $M^2_{\sigma S}$ of the Stokes beam at the output from the SBS medium.

4. Conclusions

By using the known expressions for the radius and radius of WF curvature of Stokes beams for stationary SBS obtained in the fixed-Gaussian pump beam approximation [8], we have analysed the beam size on the focusing lens and its angular divergence in front of and behind the lens. To measure accurately the radii and radii of WF curvature by the method of moments, we have proposed to produce an additional waist in the pump beam in front of the focusing lens of the SBS mirror. Then, backscattered Stokes radiation automatically forms a waist whose position and size depend on the pump-beam parameters. For nearly Gaussian focused pump beams with the propagation ratio $M^2_{\sigma p} \leqslant 1.2$, the radii and radii of curvature of Stokes beams formed upon transient SBS have been measured by the method of moments. It has been shown that upon sufficiently deep focusing of pump radiation, when the pump-beam waist in the medium is located at a distance of many diffraction lengths from the input plane of the SBS mirror, the propagation ratio $M^2_{\sigma S}$ of Stokes beams near the transient SBS threshold is lower than $M^2_{\sigma p}$ and approaches it with increasing the pump-pulse energy. It has been also found that the radii of Stokes beams at the output from the nonlinear medium are smaller than those of pump beams, and the radii of WF curvature are close (in modulus) to those of pump beams.

Acknowledgements. This work was supported by the Lithuanian Foundation for Science and Education (Grant No. 2359 CHOCLAB II, V-05048).

References

1. Zel'dovich B.Ya., Pilipetskii N.F., Shkunov V.V. *Obrashchenie volnovogo fronta* (Phase Conjugation) (Moscow: Nauka, 1985).
2. Bespalov V.I., Pasmamik G.A. *Nelineinaya optika i adaptivnye lazernye sistemy* (Nonlinear Optics and Adaptive Laser Systems) (Moscow: Nauka, 1986).
3. Basov N.G., Efimkov V.F., Zubarev I.G., Mikhailov S.I. *Trudy FIAN*, **172**, 10 (1986).
4. Sokolovskaya A.I., Brekhovskikh G.L., Kudryavtseva A.D. *IEEE J. Quantum Electron.*, **23**, 1332 (1987).
5. Ragul'skii V.V. *Obrashchenie volnovogo fronta pri vynuzhdennom rasseyanii sveta* (Phase Conjugation upon Stimulated Scattering of Light) (Moscow: Nauka, 1990).
6. Dmitriev V.G. *Nelineinaya optika i obrashchenie volnovogo fronta* (Nonlinear Optics and Phase Conjugation) (Moscow: Nauka, 2003).
7. Bal'kyavichus P.I., Dement'ev A.S., Lukoshus I.P., Maldutis E.K., Tarulis V.P. *Liet. Fiz. Rink.*, **24**, 81 (1984); Bal'kyavichus P., Dement'ev A.S., Kosenko E.K., Maldutis E. *Liet. Fiz. Rink.*, **24**, 123 (1984).
8. Kochemasov G.G., Nikolaev V.D. *Kvantovaya Elektron.*, **4**, 115 (1977) [*Sov. J. Quantum Electron.*, **7**, 60 (1977)].
9. Glazkov D.A., Gordeev A.A., Zubarev I.G., Mikhailov S.I. *Kvantovaya Elektron.*, **19**, 286 (1992) [*Quantum Electron.*, **22**, 262 (1992)].

10. Brignon A., Huignard J.-P. (Eds) *Phase Conjugate Laser Optics* (Hoboken, New Jersey: John Wiley & Sons, Inc., 2004).
11. European Standard EN ISO 11145 (November 2001).
12. International Standard ISO 11146-1 (first edition 2005-01-15).
13. European Standard EN ISO 15367-1 (September 2003).
14. International Standard ISO 15367-2 (first edition 2005-03-15).
15. Buzelis R., Dement'ev A., Vaicekauskas R., Ivanauskas F., Radavichius M. *Lithuanian Phys. J.*, **38**, 159 (1998).
16. Hodgson N., Weber H. *Optical Resonators. Fundamentals, Advanced Concepts and Applications* (London: Springer-Verlag, 1997).
17. Alda J., in *Encyclopedia of Optical Engineering* (New York: Marcel Dekker, Inc., 2003) p. 999.
18. Dementjev A.S., Iovaisha A., Shilko G., Chegis R. *Kvantovaya Elektron.*, **35**, 1045 (2005) [*Quantum Electron.*, 35, 1045 (2005)].
19. Anan'ev Yu. *Laser Resonators and the Beam Divergence Problem* (Bristol: Adam Hilger, 1992).
20. Buzyalis R.R., Girdauskas V.V., Dement'ev A.S., Kosenko E.K., Norvaishas S.A., Chegis R.Yu. *Izv. Akad. Nauk SSSR. Ser. Fiz.*, **54**, 1084 (1990).
21. Kir'yanov A.V., Aboites V., Il'ichev N.N. *J. Opt. Soc. Am. B*, **17**, 11 (2000).
22. Su H., Tang S-h., Qin Y-q., Zhang W-j., Liu A-l. *J. Opt. Soc. Am. B*, **21**, 2102 (2004).
23. Giuliani G., Denariez-Roberge M.-M., Belanger P.-A. *Appl. Opt.*, **21**, 3719 (1982).
24. Bal'kyavichus P.I., Dement'ev A.S., Kosenko E.K., Lukoshus I.P., Maldutis E.K., Tarulis V.P. *Pis'ma Zh. Tekh. Fiz.*, **7**, 385 (1981).
25. Bal'kyavichus P.I., Dement'ev A.S., Lukoshus I.P., Maldutis E.K., Tarulis V.P. *Pis'ma Zh. Tekh. Fiz.*, **8**, 816 (1982).
26. Tumorin V.V., Shklovskii E.I. *Kvantovaya Elektron.*, **31**, 203 (2001) [*Quantum Electron.*, **31**, 203 (2001)].
27. Buzelis R., Dement'ev A., Hamal K., Kubecek V., Prochazka I., Valach P. *Experim. Techn. Physik*, **4/5**, 327 (1991).
28. Buzyalis R.R., Girdauskas V.V., Dement'ev A.S., Kosenko E.K., Chegis R.Yu., Sheibak M.S. *Izv. Akad. Nauk SSSR, Ser. Fiz.*, **55**, 270 (1991).
29. Girdauskas V., Dement'ev A.S., Kairyte G., Chegis R. *Lithuanian Phys. J.*, **37**, 269 (1997).
30. Dement'ev A., Girdauskas V., Vrublevskaja O. *Nonlinear Analysis: Modelling and Control*, **7**, 3 (2002). www.lana.lt/journals/issues.php
31. Moore T.R., Boyd R.W. *J. Nonlinear Opt. Phys. Mater.*, **5**, 387 (1996).
32. Atshaarvahid S., Munch J. *J. Nonlinear Opt. Phys. Mater.*, **10**, 1 (2001).
33. Moore T.R., Fisher G.L., Boyd R.W. *J. Mod. Opt.*, **45**, 735 (1998).
34. Atshaarvahid S., Heuer A., Menzel R., Munch J. *Phys. Rev. A*, **64**, 043803 (2001).